Ion Effects in the JLEIC Electron Ring

Rui Li

JLEIC R&D meeting

4-12-18

Outline

1. Introduction
2. Ionization by the electron beam
3. Ion trapping for symmetric bunch pattern
   – Trapping condition
   – Ion distribution
   – Harmful effects on e-beam stability
4. Ion clearing by clearing gap
5. Fast beam-ion instability
6. Mitigation Methods
7. Summary

1. Introduction

- There are residual gas (H_2, H_2O, CO) in the vacuum chamber
- Scattering of the electron beam with the residual gas could cause ionization of the gas molecules
- Positively charged ions could be trapped by the electric potential of the electron beam

Introduction

- Trapped ion around the e-beam could cause emittance growth, halo formation, and coherent coupled-bunch instabilities
- Clearing gap is usually arranged to prevent ion accumulation
- For a single bunch train with clearing gap, fast ion instability could take place and cause beam size growth at the train tail
- Mitigation methods by feedback system and nonlinear optics for tune spread are usually used

2. Ionization

- Scattering of the electron beam with the residual gas (H_2, H_2O, CO) in vacuum chamber could cause ionization of the gas molecules

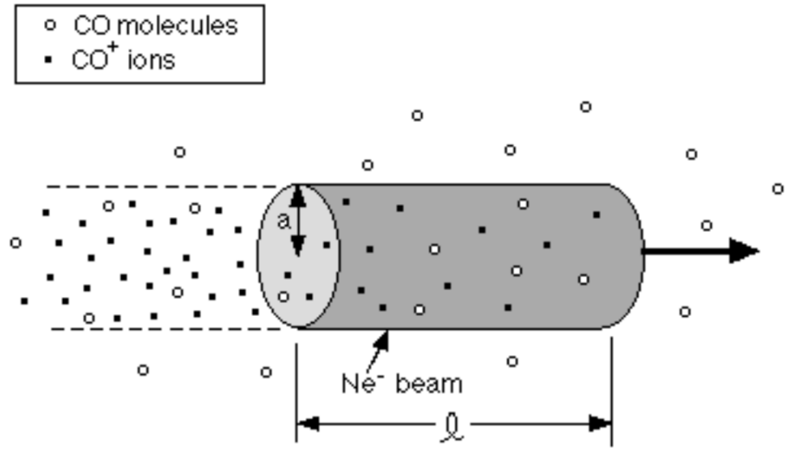

Figure 4.2: Ionization process.

- Scattering rate is proportional to the density of the residual gas

Density of Residual Gas

$$n = P / kT$$

Pressure Profile Example: Along SLC North Arc

(Emma et al, SLAC)

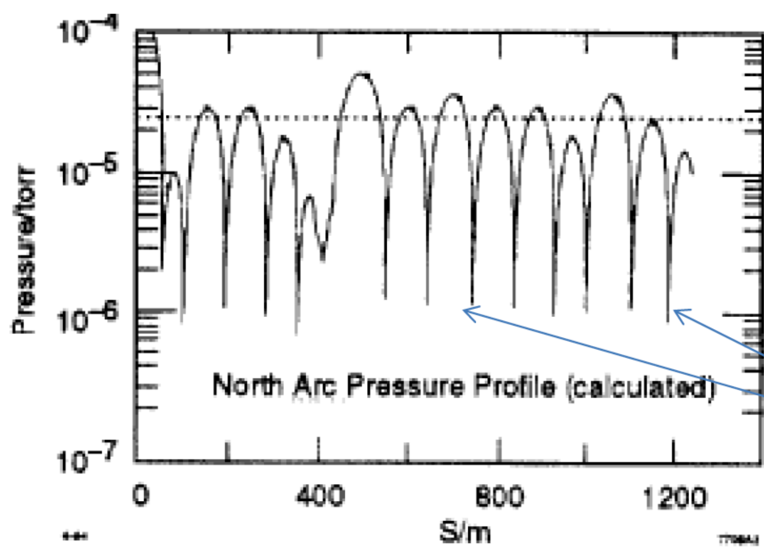

Pump locations

Figure 2: Pressure profile in the SLC north arc calculated according to [5]. The dips are the pump locations. The circles indicate newly installed vacuum gauges.

- The vacuum pressure profile is not constant throughout the arc, but exhibits variations of two orders of magnitude with sharp dips at pump locations.

Ion Species in the Vacuum

$$\lambda_i = \sigma_i N_e n_i$$

λ_i : line density of ions from N_e electrons

σ_i : scattering cross section

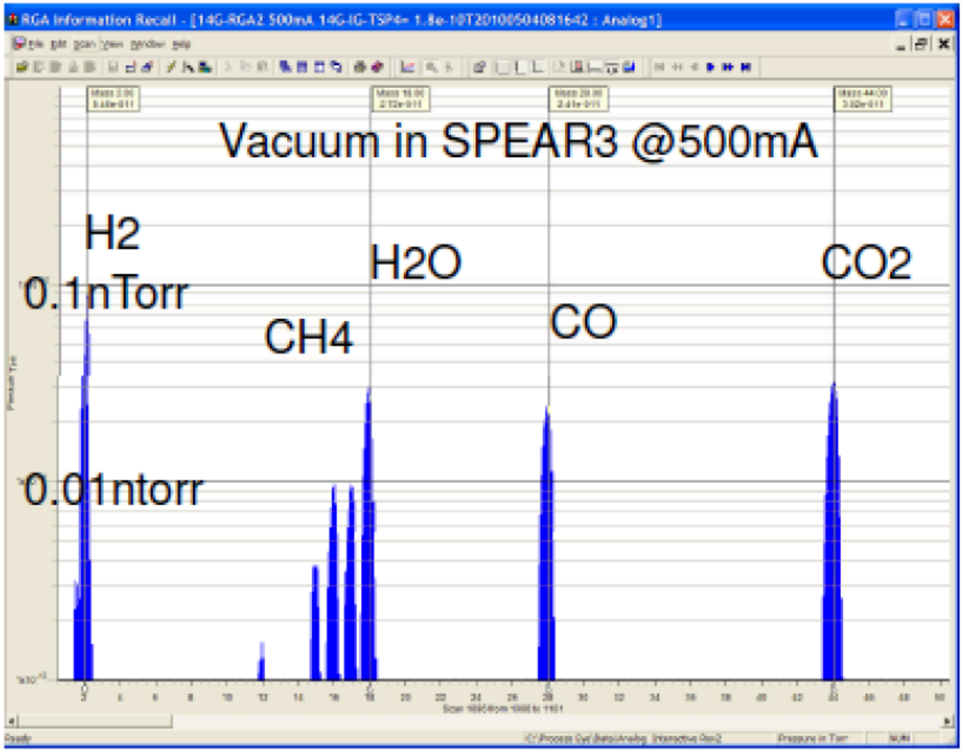

Total pressure <0.5 nTorr

Gas Species	Mass Number A	Cross-section	Percentage in Vacuum
H2	2	0.35	48%
CH4	16	2.1	5%
CO	28	2.0	14%
CO2	44	2.92	17%
H2O	18	1.64	16%

For typical ERL, H+ concentration is 90%, pressure is 1 nTorr.

Ionization Cross Section

- Ionization cross section depends on the molecule of the residual gas and on the velocity of the ionizing particle:

$$\sigma^i = 4\pi \left(\frac{\hbar}{m_e c}\right)^2 \left\{ M^2 \left[\frac{1}{\beta_e^2} \ln\left(\frac{\beta_e^2}{1-\beta_e^2}\right) - 1\right] + \frac{C}{\beta_e^2} \right\}$$

(Baconnier, CERN)

(The results were fitted to the theoretical expression by Bethe based on 1st order Born approximation)

Molecule	M^2	C	Z	A
H_2	0.5	8.1	2	2
N_2	3.7	34.8	14	28
CO	3.7	35.1	14	28
O_2	4.2	38.8	16	32
H_2O	3.2	32.3	10	18
CO_2	5.75	55.9	22	44
C_4H_4	17.5	162.4	46	76

Experimentally determined coefficients C and M^2 for different gas molecules

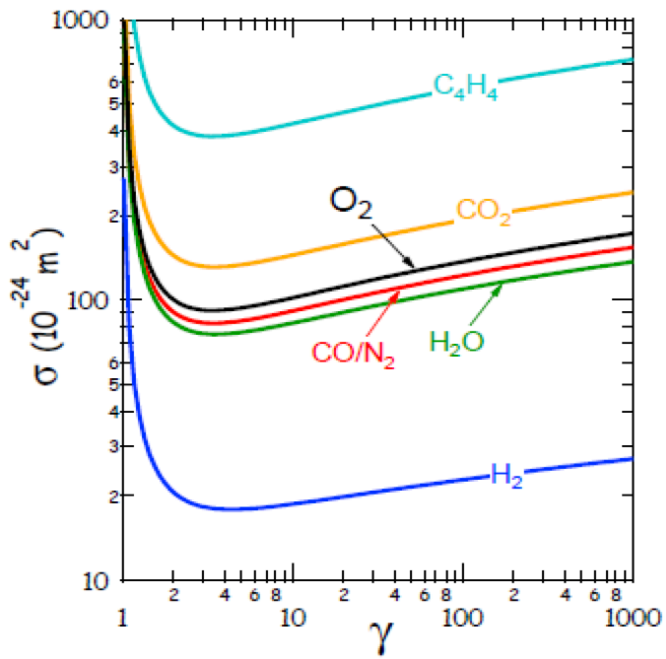

Low energy at photocathode

3. Ion Trapping for Symmetric Bunch Pattern

- Ions were born with zero velocity, and they stay in the same azimuth location s
- They see the periodic focusing e-fields of the passing-by electron bunches

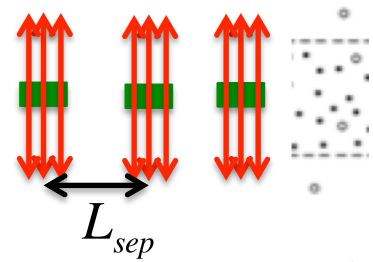

Equation of motion for the ions: $Y_1 = MY$

$$Y = \begin{pmatrix} y \\ \dot{y} \end{pmatrix}, \quad Y_1 = \begin{pmatrix} y_1 \\ \dot{y}_1 \end{pmatrix}, \quad \text{and} \quad M = \begin{pmatrix} 1 & L_{\text{sep}} \\ 0 & 1 \end{pmatrix} \begin{pmatrix} 1 & 0 \\ -k & 1 \end{pmatrix} \quad \text{for} \quad k = \frac{2N_b r_p}{A\sigma_y(\sigma_x + \sigma_y)}$$

Stability criteria: $|\mathrm{Tr}(M)| \leq 2$

or ion trapping when $A \geq A_{x,y}^{trap} = \dfrac{r_p N_b L_{\text{sep}}}{2\sigma_{x,y}(\sigma_x + \sigma_y)}$

Examples of Ion Trapping Conditions

$$\text{ion trapping when} \quad A \geq A_{x,y}^{trap} = \frac{r_p N_b L_{\text{sep}}}{2\sigma_{x,y}(\sigma_x + \sigma_y)}$$

Table 1. Storage Ring and Linac Parameters (Raubenheimer, PAC96)

	PEP-II HER	NLC DR	NLC-I pre-linac	NLC-I linac	NLC-II linac
Particles/Bunch N $[10^{10}]$	2.7	0.65	0.65	0.65	1.3
Initial Energy E_0 [GeV]	9	2	2	10	10
$\overline{\beta_0}$ [m]	15	2	13	8	8
$\gamma\epsilon_x$ $[10^{-6}$ m-rad$]$	850	3	3	5	5
$\gamma\epsilon_y$ $[10^{-6}$ m-rad$]$	34	0.03	0.03	0.05	0.05
σ_z [mm]	10	4	0.5	0.1	0.1
Bunches n_b	1658	90	90	90	90
Bunch Separation ΔL [m]	1.26	0.42	0.42	0.42	0.42
A_{trap}	0.1	14	2 at 2 GeV 10 at 10 GeV	10 at 10 GeV 50 at 250 GeV	20 at 10 GeV 140 at 500 GeV
$\hat{\mathcal{E}}$ [eV/Å]	0.0003	0.007	0.02 at 2 GeV 0.05 at 10 GeV	0.5 at 10 GeV 1.1 at 250 GeV	1.1 at 10 GeV 2.9 at 500 GeV

Comments in ICFA Beam Dynamics Newsletter

(No. 69,, pg 227)

"The serious impact of ions had even led some of the storage rings to switch the stored beam from electrons to positrons, such as DCI, ACO, APS, HERA and KEK-PF."

"With a lower beam emittance achieved as a general trend in modern storage rings to further raise the ring performance in terms of luminosity and brilliance, the trapping of ions that suffered by many rings in the past seems to have become much less of an issue because the critical mass, which represents the lightest ion that can be trapped, becomes significantly higher than known trapped species ."

JLEIC Baseline *e-p* Parameters

CM energy	GeV	21.9 (low)		44.7 (medium)		63.3 (high)	
		p	e	p	e	p	e
Beam energy	GeV	40	3	100	5	100	10
Collision frequency	MHz	476		476		476/4=119	
Particles per bunch	10^{10}	0.98	3.7	0.98	3.7	3.9	3.7
Beam current	A	0.75	2.8	0.75	2.8	0.75	0.71
Polarization	%	80	80	80	80	80	75
Bunch length, RMS	cm	3	1	1	1	2.2	1
Norm. emitt., horiz./vert.	μm	0.3/0.3	24/24	0.5/0.1	54/10.8	0.9/0.18	432/86.4
Horizontal & vertical β*	cm	8/8	13.5/13.5	6/1.2	5.1/1	10.5/2.1	4/0.8
Vert. beam-beam param.		0.015	0.092	0.015	0.068	0.008	0.034
Laslett tune-shift		0.06	7×10^{-4}	0.055	6×10^{-4}	0.056	7×10^{-5}
Detector space, up/down	m	3.6/7	3.2/3	3.6/7	3.2/3	3.6/7	3.2/3
Hourglass(HG) reduction		1		0.87		0.75	
Luminosity/IP, w/HG, 10^{33}	$cm^{-2}s^{-1}$	2.5		21.4		5.9	

(Y. Zhang, this workshop)

For the electron ring, we consider Ee=3, 5, 10 GeV
For the ion ring, we consider Ep=100 GeV (middle column)

Parameters for the JLEIC Electron Ring

Electron Ring	3 GeV	5 GeV	10 GeV
Circumference [m]		2181.39	
Pipe radius [cm]		3	
Pipe wall material		Cu	
Momentum compaction		1.09e-03	
Betatron tune (x, y)		52.7475, 52.7685	
Average beta function (x, y)		11.95, 13.15	
Number of bunches in ring	3464	3464	866
Momentum spread	2.78e-04	4.64e-04	9.28e-04
Bunch length [cm]	1.2	1.2	1.4
SR energy loss [MeVturn]	0.116	0.898	14.37
Transverse emittance [nm-rad]	2.0, 0.40	5.55, 1.11	22.2, 4.44
Transverse damping rate [1/s]	2.67	12.35	98.83
Longitudinal damping rate [1/s]	5.33	24.71	197.65
RF Voltage [MV]	0.41	2.02	17.87
# of cavities	1	2	15

(Courtesy to Fanglei Lin)

Condition for Stable Ion Motion (JLEIC e-Ring Example)

$$C = 2181.39 \text{ [m]}, \quad N_b = 3.7\times10^{10}, \quad \beta_x = 11.95 \text{ [m]}, \quad \beta_y = 13.15 \text{ [m]}$$

E [GeV]	3	5	10
n_b	3464	3464	866
L_{sep} [m]	0.63	0.63	2.52
ε_x [m-rad]	2.0	5.5	22.2
ε_y [m-rad]	0.4	1.1	4.44
ω_i [MHz]	30	18	4.5
A_x^{trap}	0.5	0.2	0.2
A_y^{trap}	1.1	0.4	0.4

(CO)

For symmetric bunch pattern, all ions (A from 2 to 44 for H_2 to CO_2) will be trapped

Distribution of the Trapped Ions

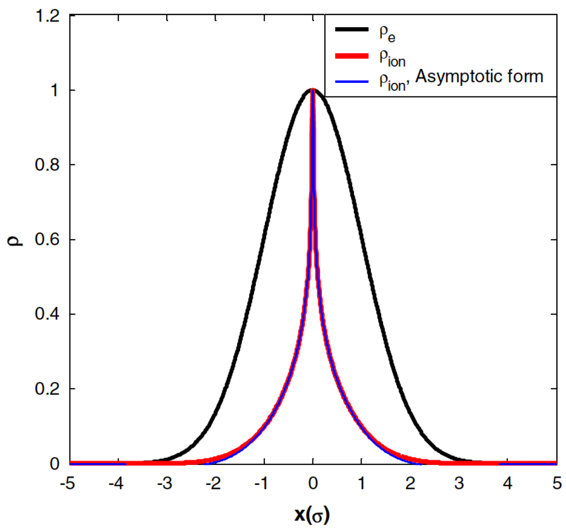

Motion of trapped ions under E-field of the electrons:

$$\begin{bmatrix} E_x \\ E_y \end{bmatrix} = \frac{eN_e}{2\pi\varepsilon_0\sigma_{e,x,y}(\sigma_{e,x}+\sigma_{e,y})}\begin{bmatrix} x \\ y \end{bmatrix}.$$

$$x(t) \approx x_0 \sin(\omega_{x0}t + \phi_0),$$

(Wang et al., PRSTAB 14, 084401)

Initial ion distribution:

$$\rho_0(x_0) = \frac{1}{\sqrt{2\pi}\sigma_{e,x}} \exp\left(-\frac{x_0^2}{2\sigma_{e,x}^2}\right).$$

Final ion distribution:

$$\rho(x) = \frac{1}{\pi\sqrt{2\pi}\sigma_{e,x}} e^{-(x^2/4\sigma_{e,x}^2)} K_0\left(\frac{x^2}{4\sigma_{e,x}^2}\right),$$

rms:

$$\sigma_i = \sigma_e / \sqrt{2}$$

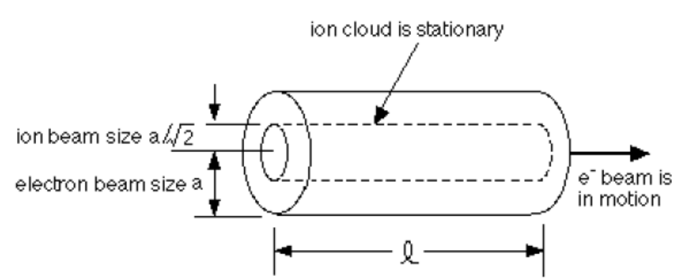

Observation of Harmful Effects from Trapped Ions

- Incoherent effects
  - Emittance growth
  - Betatron tune shifts
  - Halo formation

Vertical beam size vs. I at Spring-8

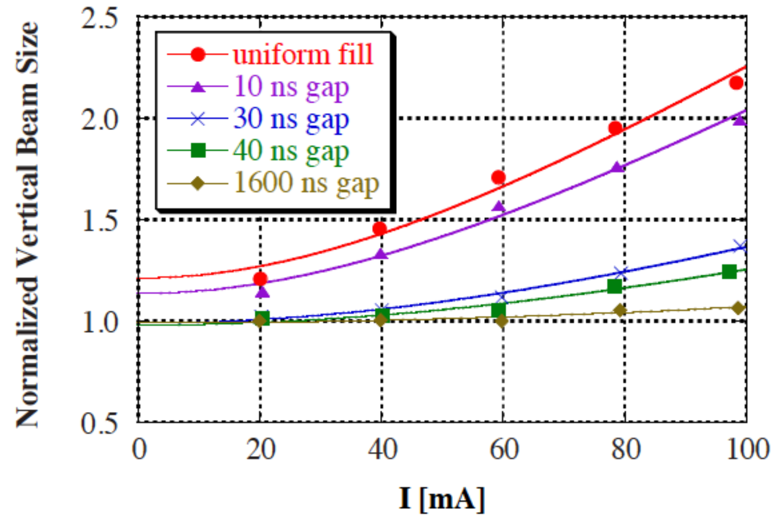

(Takao, EPAC02)

Variation of beta-y tune in Indus-2

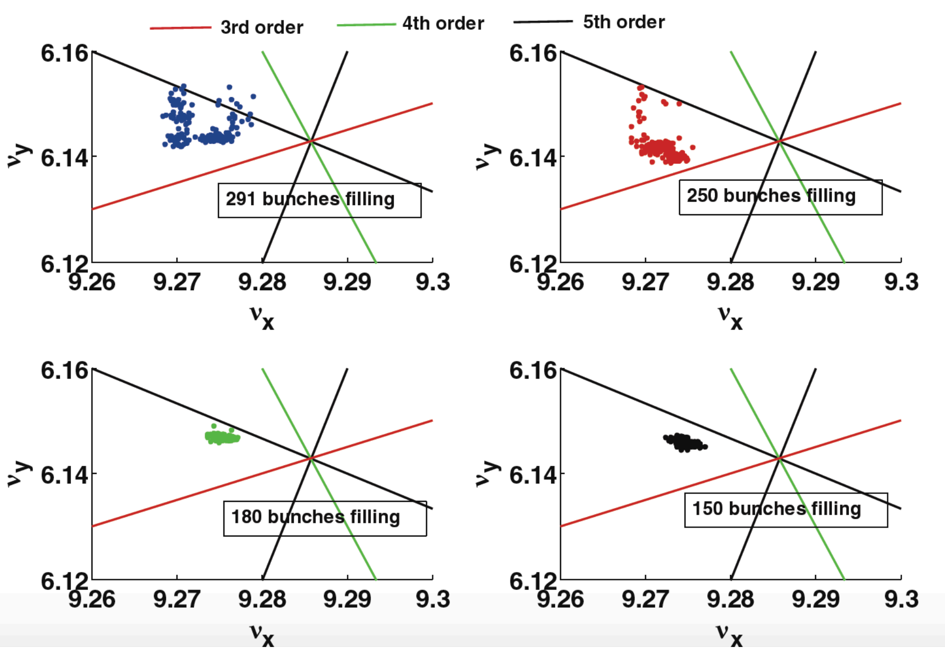

(Jena and Ghodke, J. Phys. 85, 1193)

Ion Trapping Condition along Beamline

PETRAIII Example:

$$\text{ion trapping when} \quad A \geq A_{x,y}^{trap} = \frac{r_p N_b L_{\text{sep}}}{2\sigma_{x,y}(\sigma_x + \sigma_y)}$$

- Beta function varies along the beamline, critical mass also varies along the beamline

Uniform filling by 40 bunches

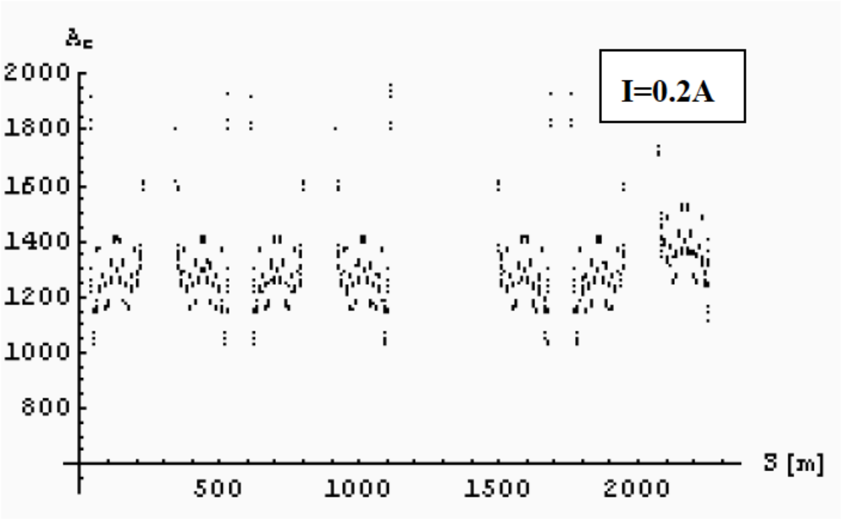

Uniform filling by 960 bunches

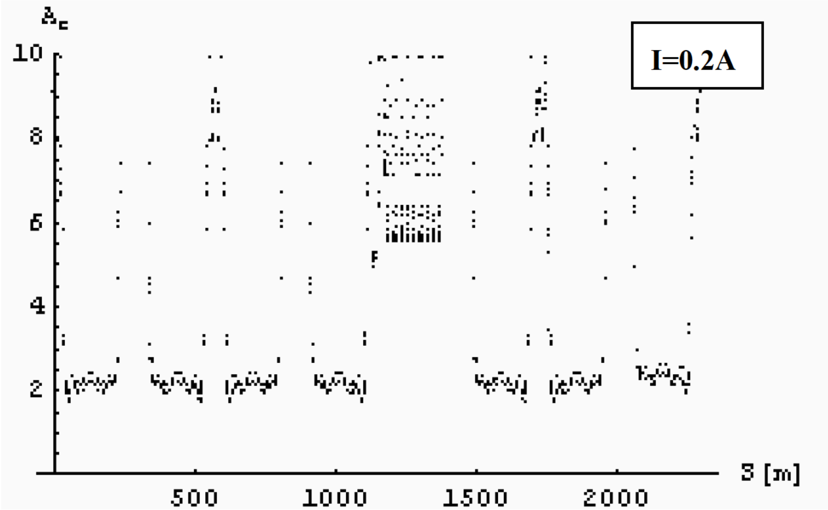

4. Ion Clearing by Clearing Gap

(Chao, SLAC-PUB-9574)

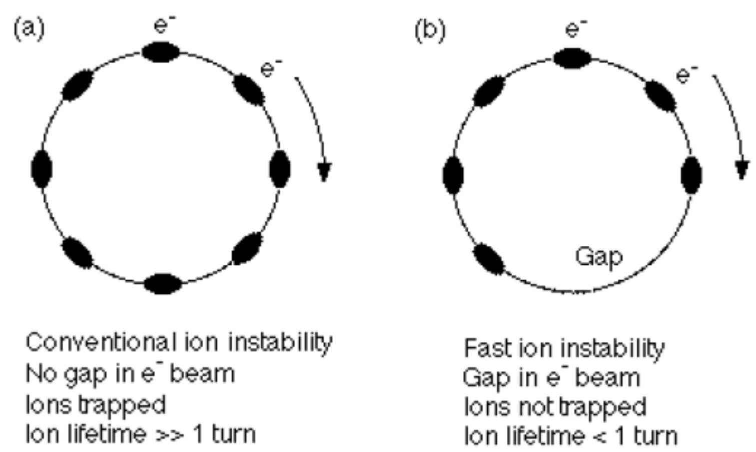

Figure 4.1: Comparison between (a) the conventional ion trapping and (b) the fast ion instability.

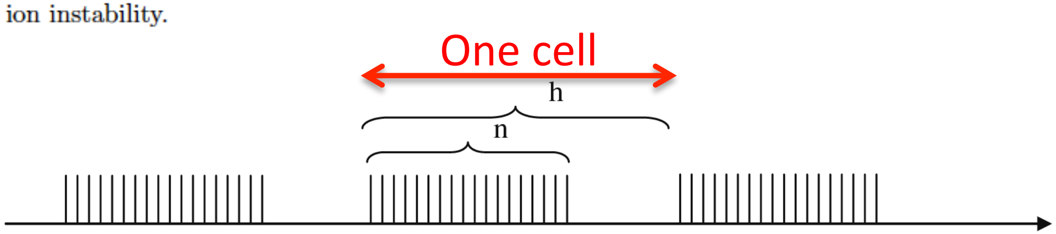

Figure 1. An illustration of the bunch train that shows a maximum possible h bunches out of which n bunches are filled with electrons and $h - n$ bunches are empty.

$$M = \left[\begin{pmatrix} 1 & L \\ 0 & 1 \end{pmatrix} \begin{pmatrix} 1 & 0 \\ -k & 1 \end{pmatrix} \right]^n \begin{pmatrix} 1 & L \\ 0 & 1 \end{pmatrix}^{h-n}$$

Stability criteria:

$$\left| \mathrm{Tr}(M) \right| \leq 2$$

Example of Stability Condition with Clearing Gap

Stable ion masses predicted by theory

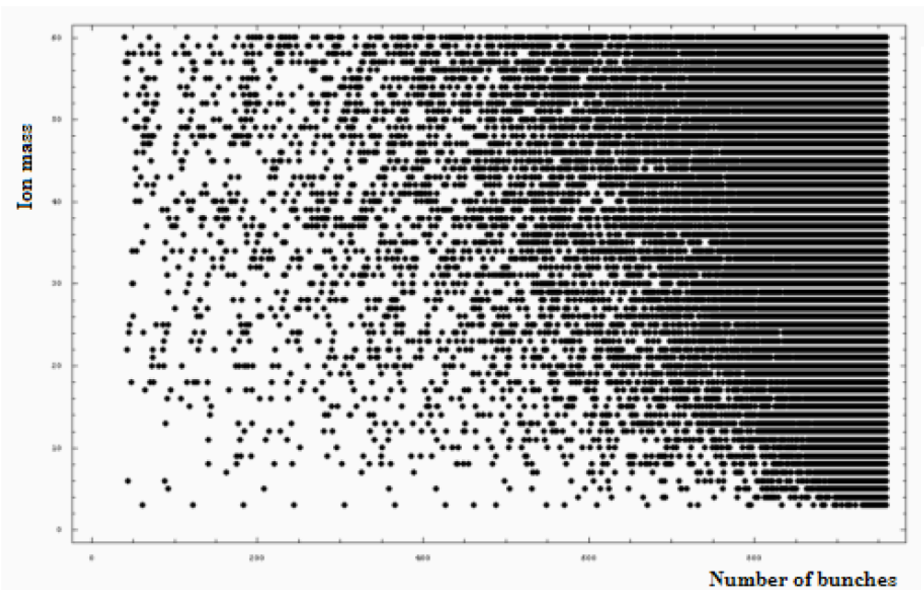

Unstable Ion numbers predicted by theory

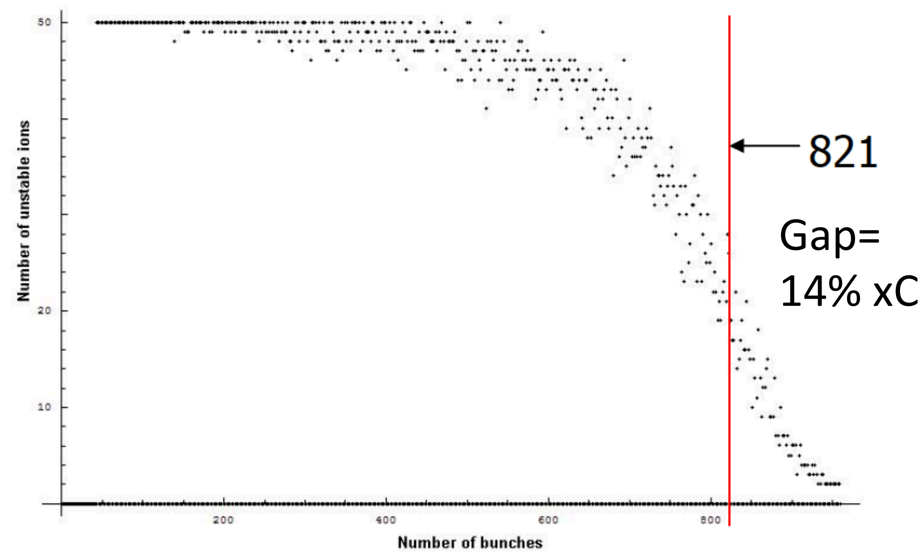

Number of bunches in the ring
out of 960 even spaces

(PETRAIII Example, Ivanyan et al., DESY M 09-01))

Stability criteria:

$$|\mathrm{Tr}(M)| \le 2$$

Stability Condition for JLEIC e-Ring (E=3 GeV)

- Ion Trapping with Clearing Gap

Ion trapped when $\boxed{\left|\mathrm{Tr}\left(M^{cell}\right)\right| < 2}$

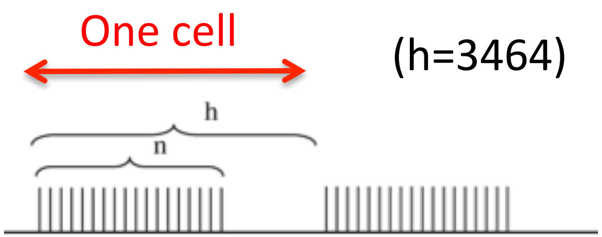

(h=3464)

x-trapped Ions, A vs. n

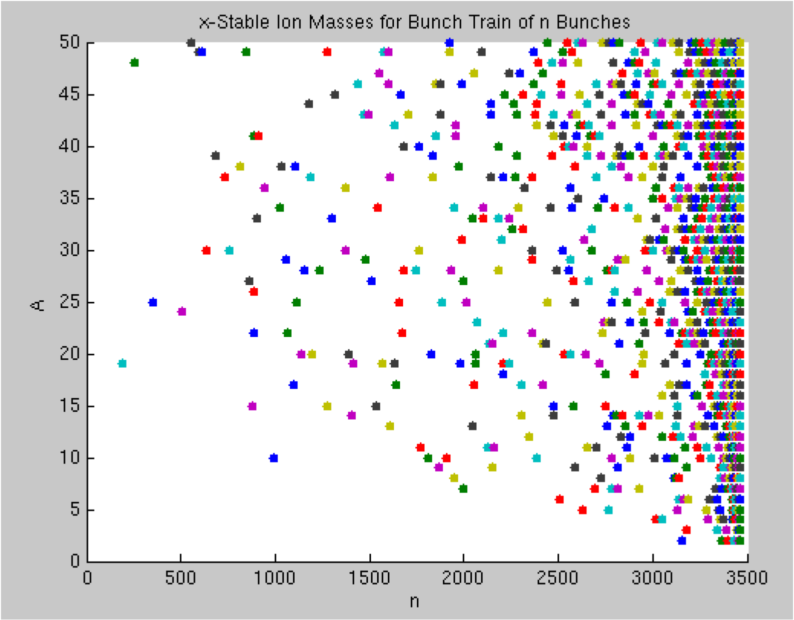

y-trapped Ions, A vs. n

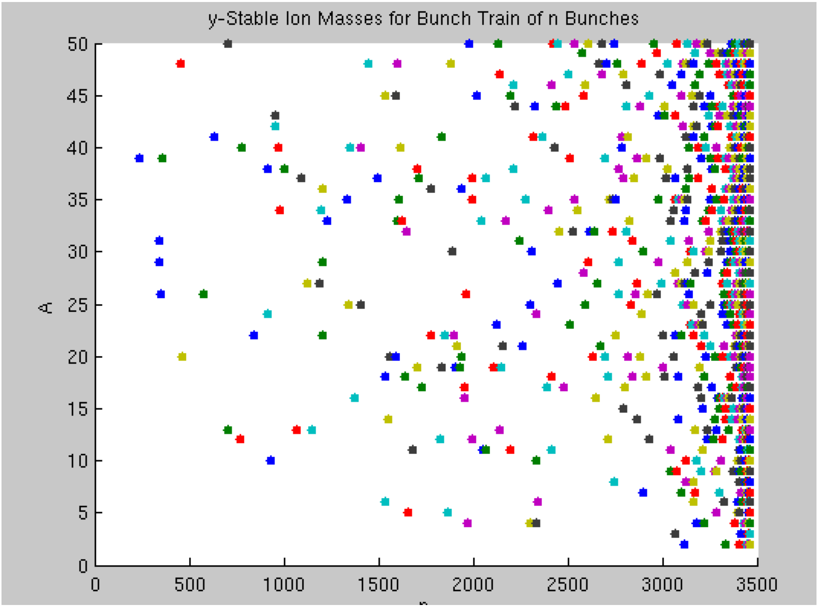

(Preliminary results, need further studies)

5. Fast Beam-Ion Instability

- Mechanism

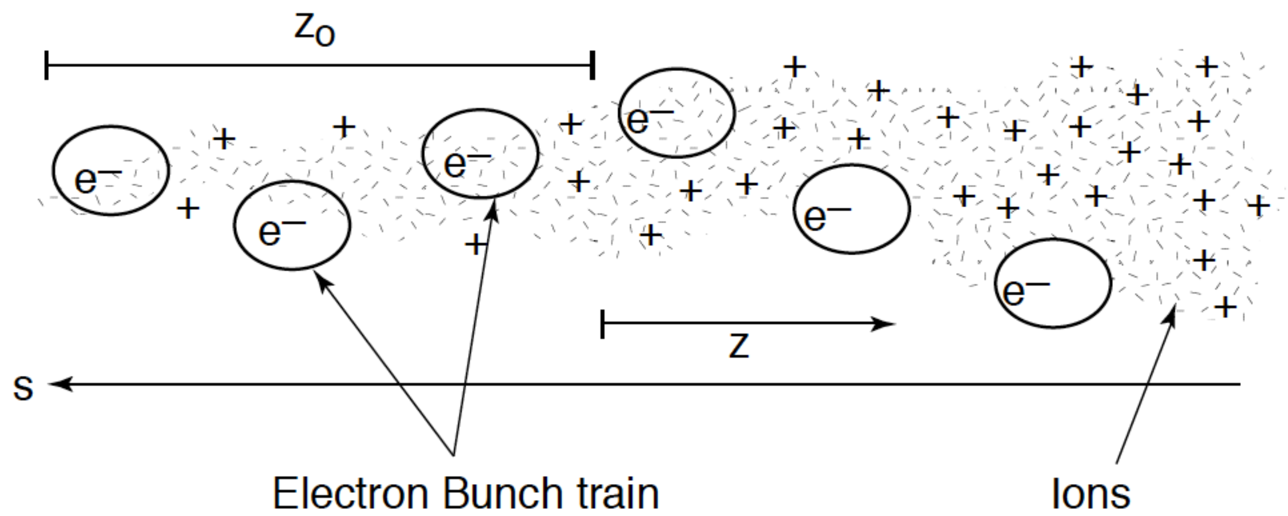

- Ions are generated by the head of the bunch and keep accumulating until they are cleared by the bunch train gap
- The ions slices will be dipole kicked by the previous electron slices and act back on the dipole motion of the trailing electron slices, serving as a transverse wakefield similar to the RF HOM wakes

Observation of the Fast Beam-Ion Instability

- Observation at NSLS2

I_{ave}=46 mA
1000 bunches

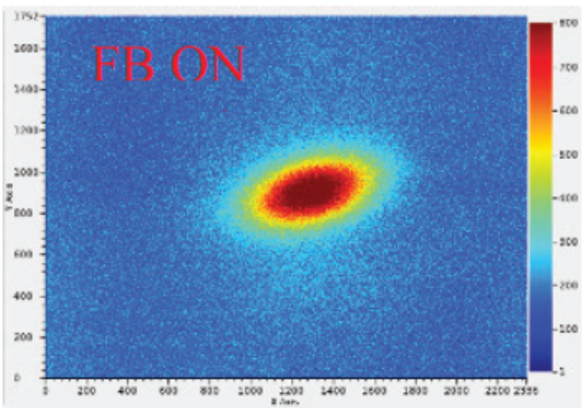

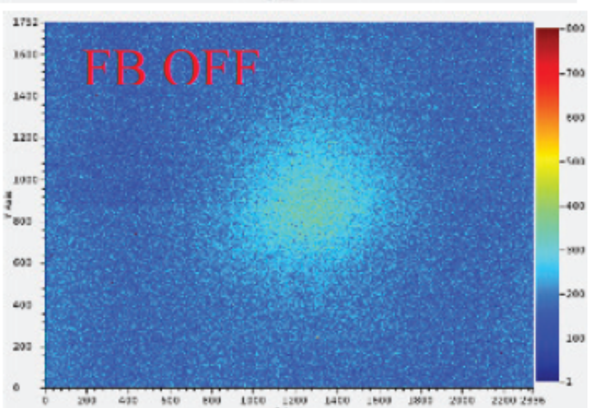

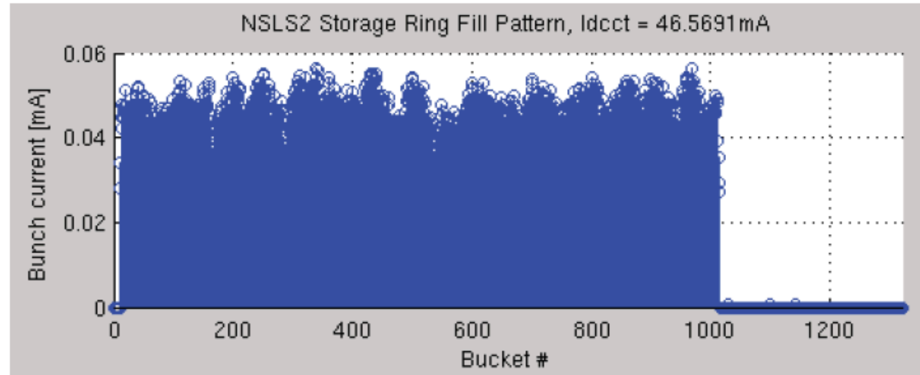

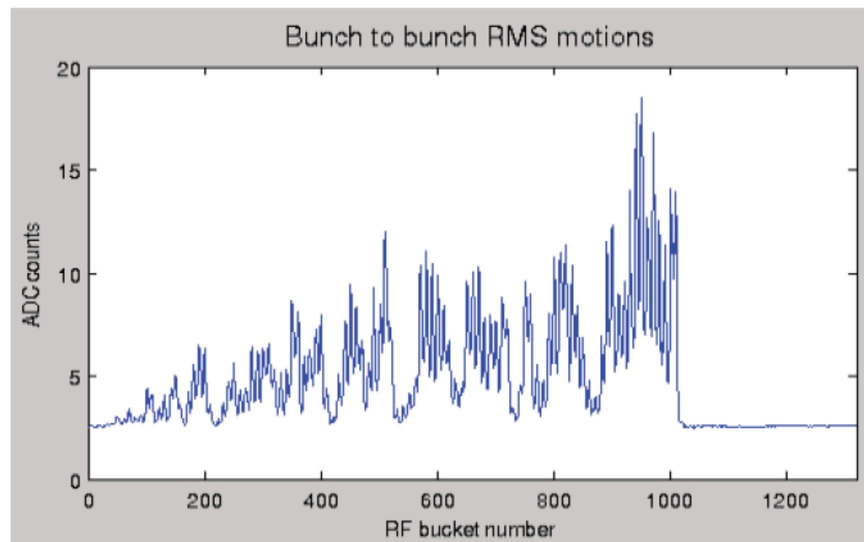

Figure 4: Bunch to bunch RMS motions along the 1000-bunch train with vertical feedback gated OFF for 20ms. Beam was filled to 46mA with all insertion devices gap closed.

Equations for the Fast Beam-Ion Instability

$$K = \frac{4\lambda_{ion}(p_{gas})r_e}{3\gamma\sigma_y(\sigma_x+\sigma_y)}$$

$$\frac{d^2 y_b(s,z)}{ds^2} + \omega_\beta^2 y_b(s,z) = K\left[y_i(s,s+z) - y_b(s,z)\right]\int_{-\infty}^{z} \rho(z')dz'$$

$$\frac{d^2 \tilde{y}_i(s,t)}{dt^2} + \omega_i^2(t-s)\tilde{y}_i(s,t) = \omega_i^2(z) y_b(s,t-s)$$

$$\omega_i = \left[\frac{4N_b r_p}{3L_{sep}\sigma_y(\sigma_x+\sigma_y)A}\right]^{1/2}$$

(Raubenheimer and Zimmermann, PRE 52)

Growth Time for JLEIC e-Beam

$$\tau_{inst}^{-1}\left[s^{-1}\right]=5p\left[Torr\right]\frac{N_b^{3/2}n_b^2 r_e r_p^{1/2} L_{sep}^{1/2} c}{\gamma\sigma_y^{3/2}\left(\sigma_x+\sigma_y\right)^{3/2} A^{1/2}\omega_\beta}$$

$$y_b(t)\propto e^{\sqrt{t/\tau_{inst}}-t/\tau_{damp}}$$

For A=28

	PEPII HER	JLEIC e-Ring		
E [GeV]	9	3	5	10
N_b	$3x10^{10}$	$3.7x10^{10}$		
n_b	1658	3464	3464	866
L_{sep}	1.26	0.63	0.63	2.52
β_y [m]	15	13.15		
σ_x [mm]	1.06	0.15	0.26	0.51
σ_y [mm]	0.17	0.07	0.12	0.24
τ_{inst} [μs]	6.8	0.01	0.11	13.9

Typical feedback system: $\tau_{damp}\approx 1$ [ms]

Limitation of the Theory

- Assumes linear force between beam and ions
- Ignores Landau damping by lattice and beam-beam induced tune spread
- Ion frequency is treated as constant, but it would vary along the beamline
- Smooth approximation of the ion oscillation, not beam-gap periods.
- Ionization could also be generated by synchrotron radiation

Various Time Constant for FBII

- Simple linear model $(|y| < \sigma_y)$

$$y \approx \hat{y} \frac{1}{2\sqrt{2\pi}(t/\tau_c)^{1/4}} \exp(\sqrt{t/\tau_c})$$

$$\frac{1}{\tau_c} \equiv \frac{4 d_{gas} \sigma_{ion} \beta N_b^{3/2} n_b^2 r_e r_p^{1/2} L_{sep}^{1/2} c}{\sqrt{3}\, 3 \gamma \sigma_y^{3/2} (\sigma_x + \sigma_y)^{3/2} A^{1/2}}.$$

- Including frequency spread (e-folding time)

$$y \sim \exp(t/\tau_e)$$

$$\frac{1}{\tau_e} \approx \frac{1}{\tau_c} \frac{c}{4\sqrt{2}\pi L_{sep} n_b a_{bt} f_i},$$

- Large amplitude $(|y| \gg \sigma_y)$

$$y \sim \sigma_y \frac{t}{\tau_H}$$

$$\frac{1}{\tau_H} \approx \frac{1}{\tau_c} \frac{c}{2\pi f_i L_{sep} n_b^{3/2}}$$

Example of Various Time Constant for FBII

accelerator	ALS experiment	PEP-II HER
ϵ_x^N [μm]	12	500
ϵ_y^N [μm]	0.4	25
n_b	$160, \mathbf{240}, 320$	1658
N_b [10^{10}]	0.4–0.8	3
$\beta_{x,y}$ [m]	$2.5, 4$	$25, 20$
σ_x [μm]	200	1250
σ_y [μm]	20	200
L_{sep} [m]	0.6	1.2
E [GeV]	1.5	9
p [nTorr]	$80^{\ddagger}$	5^{*}
f_i [MHz]	$40^{\ddagger}$	4^{*}
$4L_{sep}f_i/c$	0.34	0.15
ΔQ_y [10^{-3}]	3.2	6.1
τ_c [μs]	0.4	2
τ_e [μs]	14–140	74–740
τ_H [ms]	0.76	10.7

Table 3: Parameters and predicted oscillation growth rates for the ALS machine experiment compared with those for the PEP-II High-Energy Ring.
‡for helium atoms; *assuming carbon-monoxide or nitrogen molecules.

The time constant could be differ by orders of magnitude!

Early Observation of FBII at ASL

TFB on

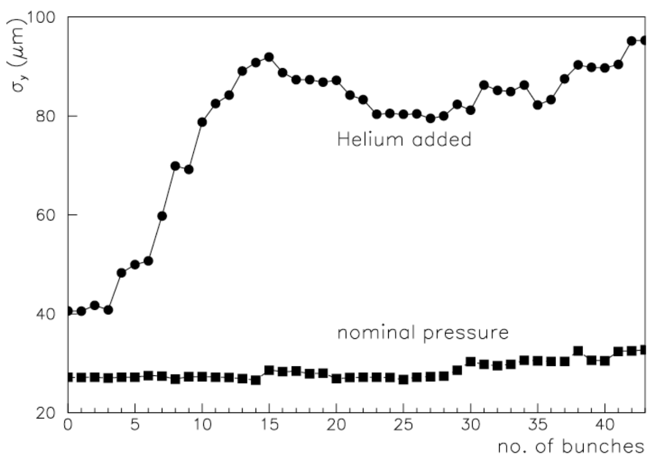

TFB off

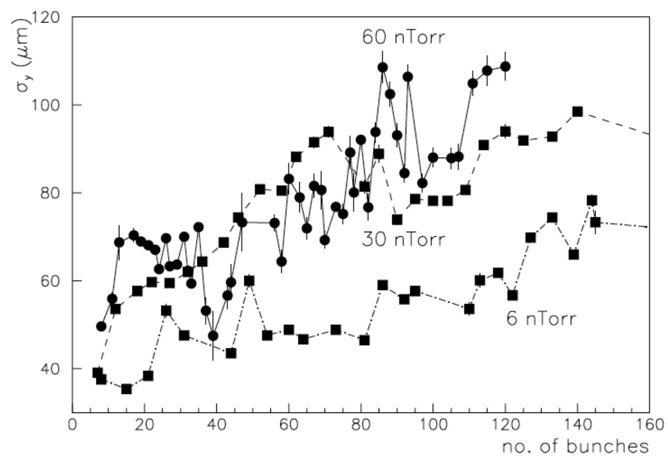

Figure 1: *RMS vertical beam size versus the number of bunches at a current of 0.5 mA/bunch: (left) for nominal and elevated pressure conditions, TFB on; (right) for three different values of the average helium pressure, TFB off.*

Recent Observation of FBII at CESR-TA

- Three pressures of Kr of 10, 17 and 25 nTorr were established
- Solid==Feedback on, Lightly Shaded==feedback off

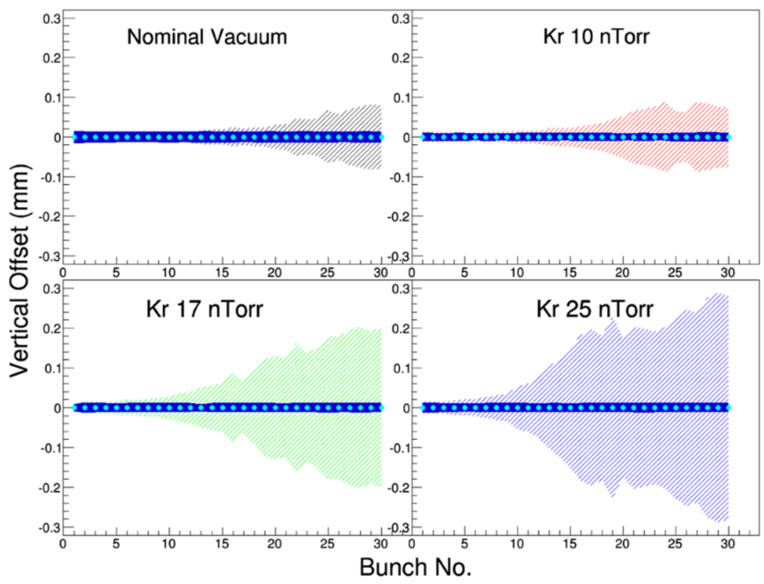

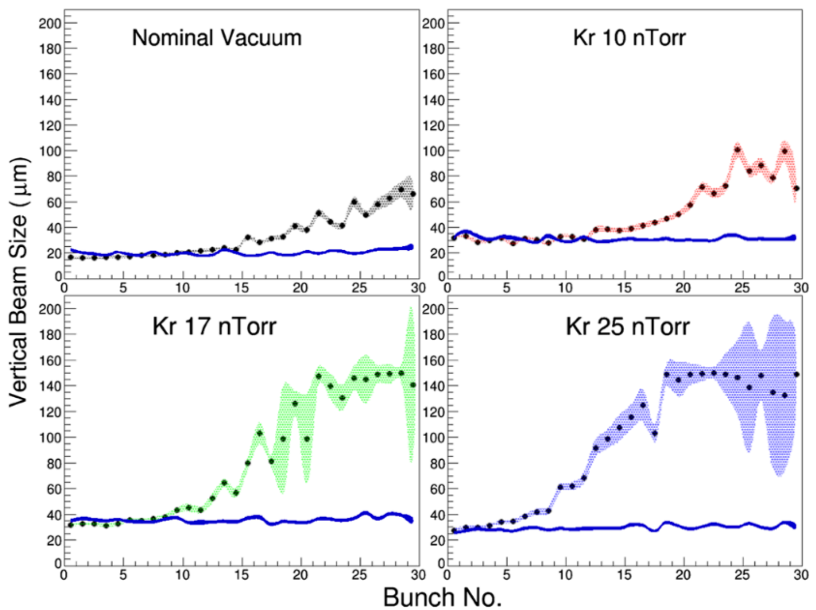

(Chatterjee, PRSTAB, 2015)

PEPII Observations

- Originally envisioned gap: 10% (about 120 buckets)
- In real operation, abort-kicker gap: 18 buckets (about 100ns)
- With 16 bucket gap, instability takes place---unstable when colliding, and stable otherwise

The previously concerned effect could be shifted due to the combined action of the transverse bunch-by-bunch feedback and the Landau damping from the beam-beam interaction

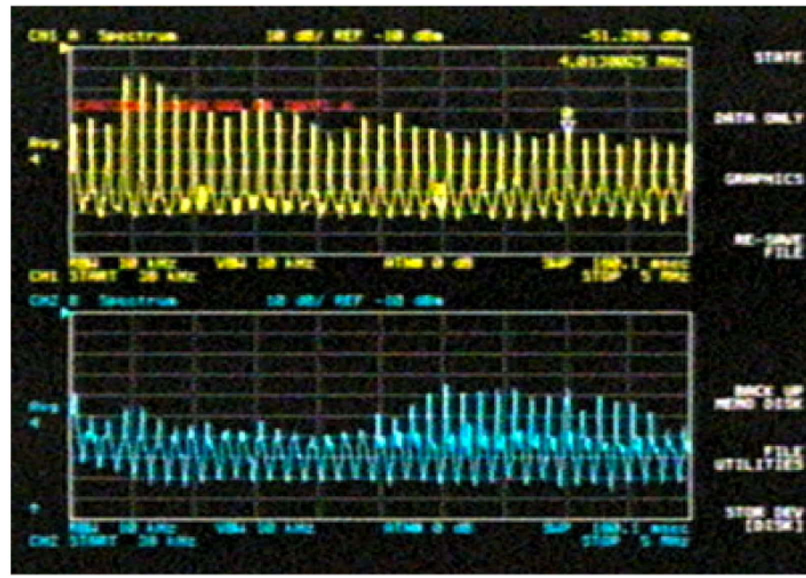

Fast ion instability

Figure 7: Transverse spectra of the HER with 16-bucket gap (34 ns). Top trace (yellow) is horizontal; bottom trace (blue), vertical motion. The frequency range is from 20 kHz to 5 MHz and the vertical scale is 10 dB/div in both spectra.

(Wienands, EPAC08)

EFFECT OF IONS IN THE HER

While initially a concern, ion effects in the HER have not been a significant limitation to operation of PEP-II. In fact, the machine had been run with the abort-kicker gap reduced to about 1.4% (18 buckets or about 100 ns), down from the originally envisaged 10%. Since the gap in the beam leads to significant phase transients—which cause difficulties for the rf system—an experiment was conducted to explore reducing the gap to its minimum size and, potentially, omitting the gap completely. The experiment had the surprising outcome that in fact we could not reduce the gap by any significant amount without causing trouble. By the time the gap was reduced to near 1% clear signs of beam motion were observed and luminosity had in fact not increased. Further reduction in the gap lead to outright beam instability and reduction of luminosity. The motion occurred in both planes and the vertical motion exhibited enhanced spectral content around 2…4 MHz, see Fig. 7. This sig-

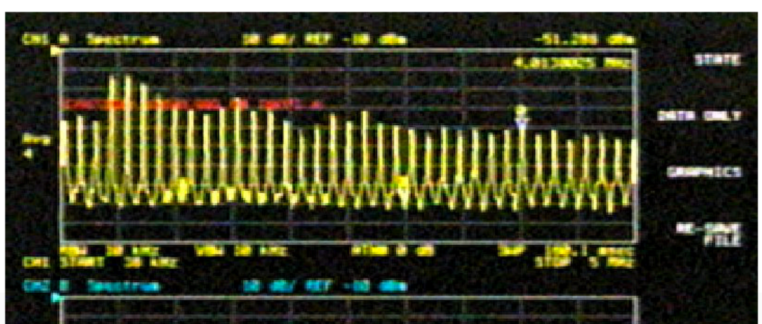

Ion Effect at SUPERKEKB (predicted)

(D. Zhou, 2013 SUPERKEK Review)

5. Fast ion: HER: Simulation results (L. Wang)

- Vertical growth time: τ_y = 44μs for $P_{tot}=5\times10^{-7}$Pa
- If total pressure $P_{tot}=1.3\times10^{-7}$Pa(1 nTorr), τ_y = 104μs
- If H_2 is dominant(e.g. 70%), as expected in long term operation, τ_y = 76μs ($P_{tot}=5\times10^{-7}$Pa)

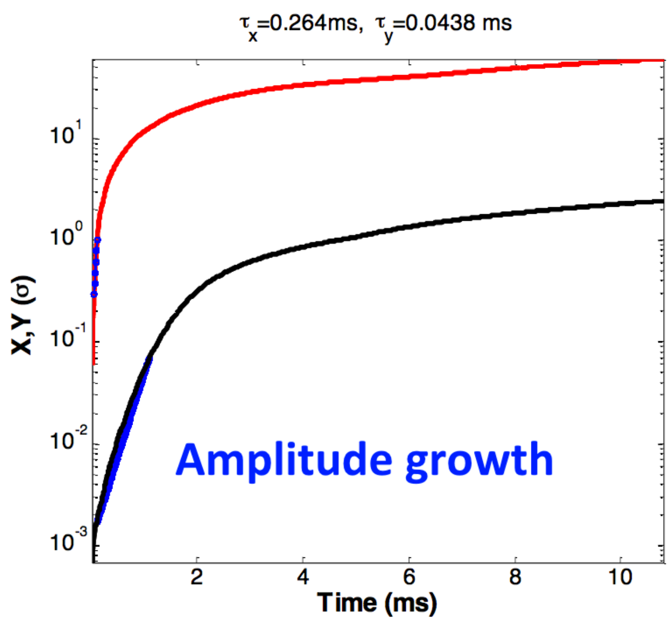

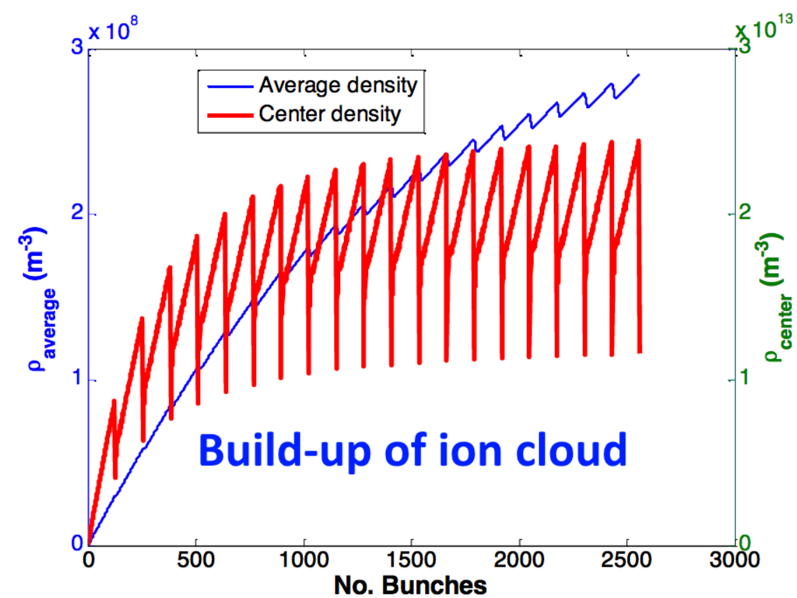

L. Wang and H. Fukuma

Ion Effect at SUPERKEKB

(D. Zhou, 2013 SUPERKEK Review)

- **BBWS: Lum. loss < 10% ➡ DY/σ_{y0} < 5%**
- **Future study:**
  - **Optimum fill pattern**
  - **Expected pressure**
  - **Bunch feedback**

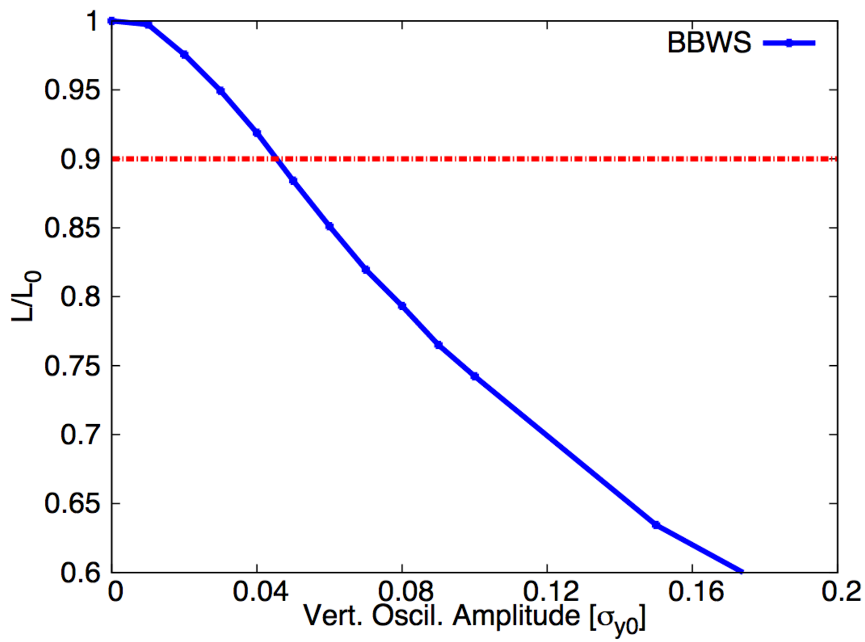

Ion Effect at SUPERKEKB (measured)

(Ohmi, IPAC2017)

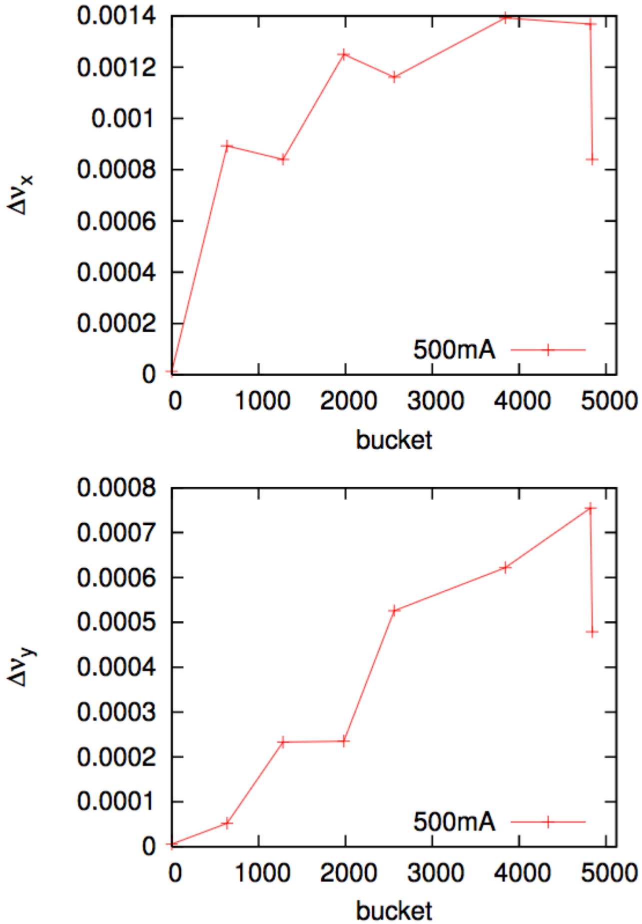

Figure 3: Horizontal (top) and vertical (bottom) tune shift along the bunch train.

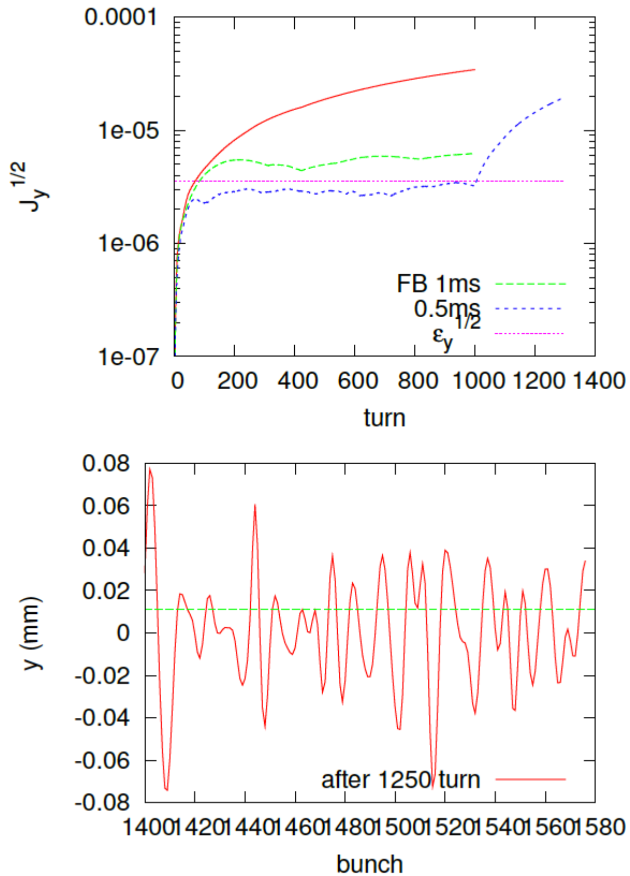

Figure 5: Ion instability in the experimental condition, N_b 1576, 3 bucket spacing, I = 500 mA, 100 nPa.

- Unsolved phenomena remain

6. Mitigation Method

- good vacuum
- uneven bunch filling
- Clearing electrode for ion stripping
- ion shaking
- Chromaticity
- Feedback system for fast ion instabiilty

Examples of Mitigation

- ASL Experiment

(Zimmermann, SLAC-PUB-7736)

σ_y vs. ξ

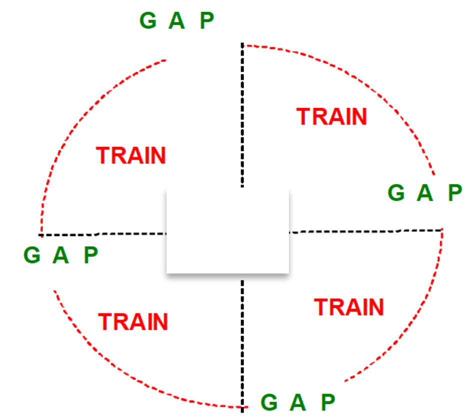

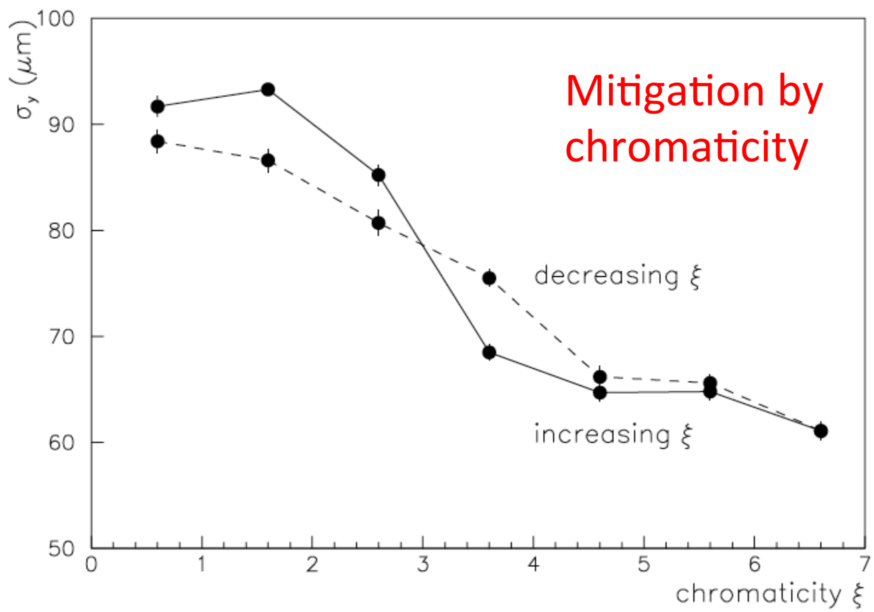

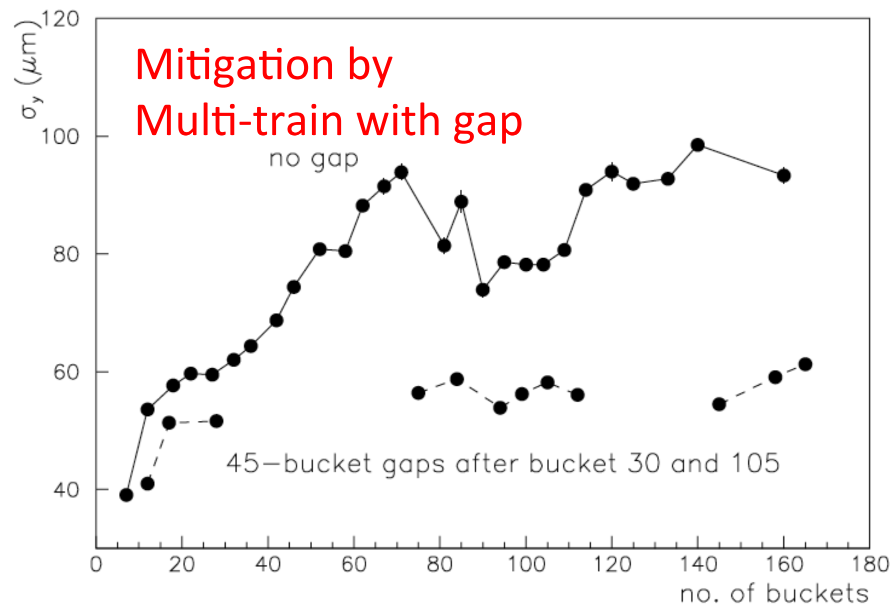

7. Summary

- For JLEIC e-ring, all ions will be trapped if with even bunch filling
- A clearing gap can help, and PEPII HER experience tells that the gap can be much shorter than previously envisaged
- The fast beam-ion instability for JLEIC can have very fast growth time. For low energy, this instability could be of serious concern. Much more careful studies are required.
- However, from PEPII experience, the beam-beam effect can serve as Landau damping for the instability. We need to study the combined effects in order to get any conclusive prediction

References

- T. O. Raubenheimer, “Ion effects in future circular and linear accelerators”, pg. 2752, PAC1996.
- S. Jena and A. D. Ghodke, “Observation and mitigation of ion trapping in Indus-2”, Pramana – J. of Phys., Vol. 85, No. 6, 1193 (2015).
- W. Cheng, et al., “Observation of Ion-induced instabilities at NSLS2 storage rings”, IBIC2015.
- U. Wienands et al., “High-current effects in the PEP-II storage rings”, EPAC02, pg. 2611.
- Heifets, “Beam-Ion Instability in PEP-II”, SLAC-PUB-12959.
- D. Zhou, “Beam dynamics in SuperKEEB”, 2013.